

Section 2 PROGRESS IN LASER FUSION

2.A High X-Ray Conversion Efficiency with Target Irradiation by a Frequency Tripled Nd:Glass Laser

Recently the high efficiency frequency tripling of a high power Nd:glass laser has been demonstrated.^{1,2} The single beam GDL laser system produces pulses of peak power 0.1–0.2 TW at a wavelength of 0.35 μm . Using this laser we measured x-ray production from various plane targets irradiated by short (100 psec) and long (500 psec) UV pulses where the flux on target was varied in the range 10^{13} – 10^{15} W/cm² by changing the beam spot size on target.

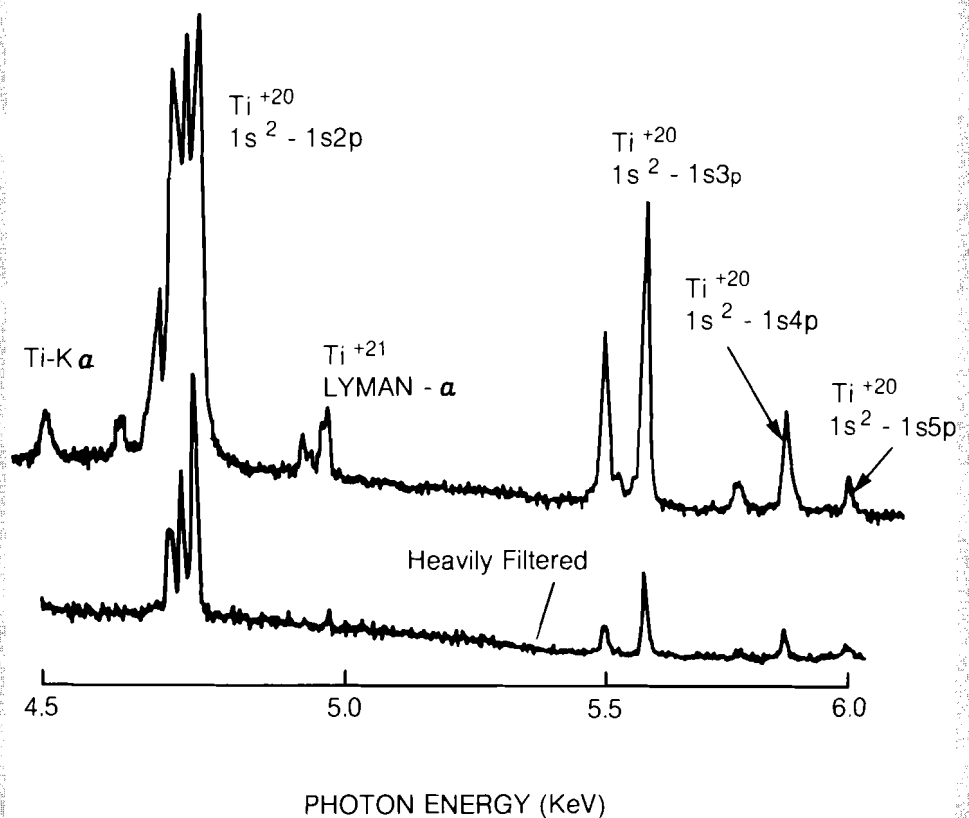
The determination of x-ray yield from UV laser-irradiated targets is of interest both in obtaining a signature of the efficiency of coupling laser energy into the target as well as in assessing the target usefulness as an intense x-ray source for probing other samples. Short wavelength lasers ($\lambda < 0.5 \mu\text{m}$) are currently strongly favored as drivers in fusion studies primarily because of their superior coupling to the target.³ This means higher absorption and a smaller fraction of the absorbed energy which goes into fast electrons. Both of these factors lead to better coupling into the thermal plasma component and should result in a higher intensity of x-rays in the energy range of a few KeV. Indeed we find that for a comparable irradiance on target, tripling the laser frequency leads to about an order of magnitude higher x-ray yield in this photon energy range.

The application of x-rays from a laser target as a probe of *transient* phenomena has recently received increasing attention.

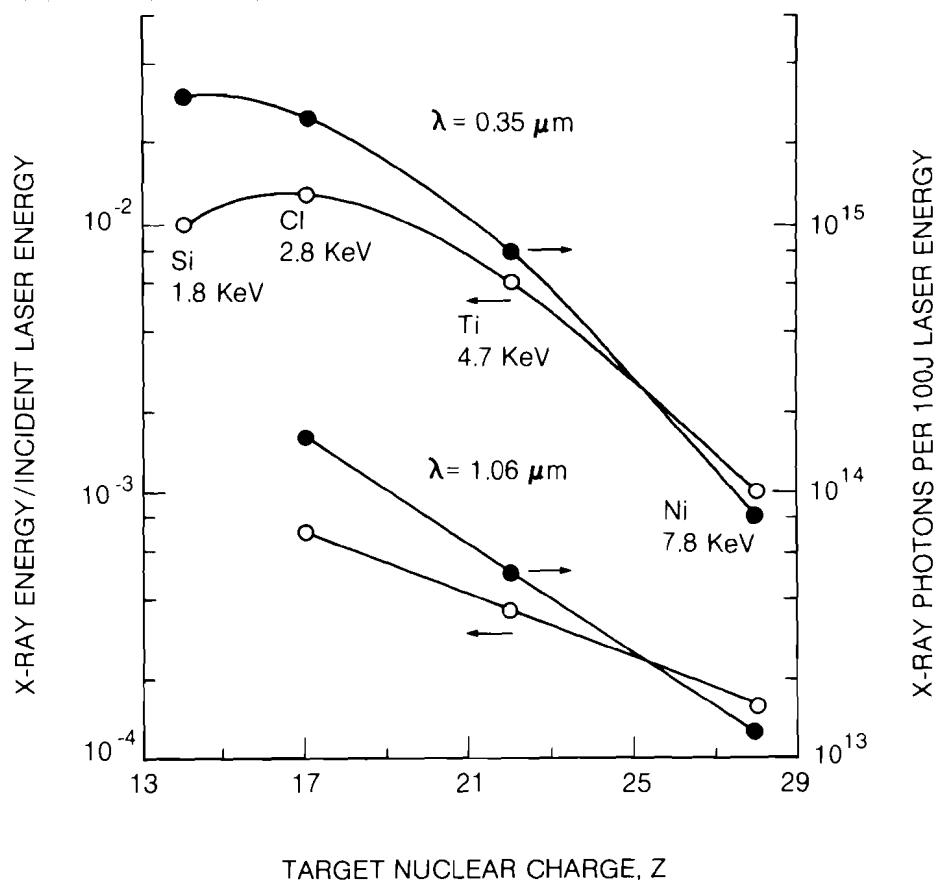
X-ray radiography (back-lighting) is being developed as perhaps the most promising way for diagnosing cold, highly-compressed laser targets.⁴ X-rays from laser targets have also been used recently to record the diffraction pattern from a crystal protein⁵ and the K-edge fine-structure absorption spectrum of sulfur in a Gypsum crystal.⁶ Finally, x-ray pumping leading to lasing in the soft x-ray region has been under active study, employing either resonant or photo-ionization type pumping.⁷ In all of these areas the intensity of the x-ray source has been the factor limiting significant progress; the advent of frequency up-converted high power lasers thus opens new possibilities. In some of these applications a quasi-monochromatic source is required (radiography, diffraction, resonant pumping) whereas the others require a wide-band continuum source. We find that both lines and continuum increase significantly in intensity in going from infrared to ultraviolet target irradiation. Furthermore, over the parameter ranges studied, the x-ray intensity was found to depend almost exclusively and nearly linearly on the total laser pulse energy.

Fig. 11
 X-ray spectrum emitted from titanium target irradiated by a 0.35 μm laser (5 × 10¹⁴ W/cm², 500 psec). Lower trace shows the simultaneously obtained spectrum through a 15 μm thick aluminum foil. The filtered spectrum allows the determination of exposure far below the intensity range of film saturation.

The flat targets used in this study (of size 2 × 2 mm and thickness 0.2 mm) were glass, saran, titanium, and nickel. X-ray line spectra



E1242



E1239

Fig. 12

Quasi-monochromatic x-ray conversion efficiency versus the nuclear charge Z of the emitting ion. X-ray emission into 4π refers to the resonance line $1s^2-1s2p$ of the helium-like ionization state including the nearby dielectronic satellite and intercombination lines (Si lines also include the resonance line of the hydrogen-like ionization state). The targets used to obtain these points were: glass, saran, titanium and nickel. The corresponding laser pulse parameters: upper curves: 40 J, 500 psec, 5×10^{14} W/cm²; lower curves: 175 J, 800 psec, 10^{15} W/cm².

of the helium-like and hydrogen-like ionization states of the elements Si, Cl, Ti, and Ni were recorded. Gypsum, P.E.T., germanium, and LiF crystals were used alternatively to record the respective spectra. The diffraction curve and hence the integrated reflectivity of each of them was measured for a set of wavelengths at the National Bureau of Standards. The spectrometer viewed the target at an angle of 45° with respect to the laser beam direction (and the normal to the target). Silicon spectra were recorded on Kodak RAR-2497 film, all other spectra were taken on Kodak No-Screen Medical x-ray film. These films were calibrated using continuous x-ray sources and the results agree well with published data.^{8,9}

Figure 11 shows as an example the spectrum obtained from a titanium target irradiated with 40 J, 500 psec pulse focused with an f/12 lens to give an irradiance of about 5×10^{14} W/cm². The lower trace shows the spectrum attenuated by a 15 μ m thick aluminum foil, obtained simultaneously. The filtered spectrum allows the determination of exposure far below the intensity range of film saturation. The spectrum consists mostly of lines,

the only significant continuum appearing in the lower-Z Si and Cl spectra beyond the series limit (see below). To obtain quasi-monochromatic radiation a titanium filter can be used; its K-edge is slightly above the $1s^2-1s2p$ line thus attenuating strongly the higher energy lines but hardly affecting the intense resonance transition (all elements with $Z > 16$ have this property). We therefore consider the integrated intensity of the resonance line $1s^2-1s2p$ of Ti^{+20} along with the adjacent weaker lines, the intercombination lines $1s^2-1s2p$ 3P , and a blend of dielectronic satellites. For Ni these normally weaker lines become more intense than the resonance line. Figure 12 shows the intensity of the comparable transitions of the helium-like ionization state of Si, Cl, Ti, and Ni. For Si we added the intensity of the Lyman- α ($1s-2p$) line of Si^{+13} which is more intense than the $1s^2-1s2p$ line of Si^{+12} , and which cannot be removed using the foil filtration technique described above. The experiments involving glass, saran, and nickel targets had similar irradiation conditions to those of titanium (Fig. 11). The results in Fig. 12 were obtained from the measured intensities by integrating over the full solid angle, assuming spherical symmetry. If the source angular distribution is Lambertian instead, its average intensity will be very close to that at 45° to the surface normal, where the spectrograph was actually located. For the applications listed above one is mostly interested in the intensity per unit solid angle in a given direction. The precision in this quantity is limited by uncertainties in the film calibration curves which we estimate to be within a factor ~ 1.5 based on comparing our calibration with published results.^{8,9}

Short laser pulses (100 psec, 0.2 TW) produced nearly the same x-ray conversion efficiency as longer pulses for Si through Ni. Defocusing the laser to lower the irradiance by more than an order of magnitude typically increased the conversion efficiency by a factor < 1.5 . All this indicates that x-ray yield scales primarily with total laser pulse energy, at least within the present parameter range. The fact that large focal spots produce more, not less, total emission is favorable for back-lighting where the source angular size has to exceed that of the probed target.

Figure 12 compares these results with x-ray yield data obtained from the same laser operating at $1.054 \mu\text{m}$. Its output energy was boosted by four active mirrors¹⁰ to produce 700 psec pulses of 175 J energy. An f/4 focusing lens produced an irradiance of 10^{15} W/cm^2 . As seen in Fig. 12, UV irradiation is more efficient in producing x-rays, by a factor of order 10 which decreases with increasing Z. This observation at high Z is believed to be due to the significant presence of fast electrons in IR laser irradiation which can contribute to the excitation of high energy x-ray lines.

In addition to lines, the spectra also display continuum radiation due to recombination; bremsstrahlung radiation is much weaker. As an example we show in Fig. 13 the free-bound continuum due to the recombination process $e^- + Si^{+14} \rightarrow Si^{+13} + h\nu$. The continuum fluence is expressed in terms of KeV/KeV, the

numerator refers to the intensity of the radiation, the denominator to the spectral interval. This unit is numerically equal to the number of photons per energy interval $\Delta E = E$. Again, this fluence is higher by about an order of magnitude than for comparable IR laser irradiation. Integrated over its spectrum ($E > 2.7$ KeV), the total continuum fluence amounts to 2×10^{15} photons, about equal to the number of photons in the $1s^2 - 1s2p$ resonance line. Similar intensities of Si continuum have previously been obtained with 100 J pulses of a six beam laser ($\lambda = 1.06 \mu\text{m}$) which symmetrically irradiated and compressed spherical targets.⁶ However, continuum intensity comparable to that in Fig. 13 could only be achieved with targets which were optimized for a high density implosion.

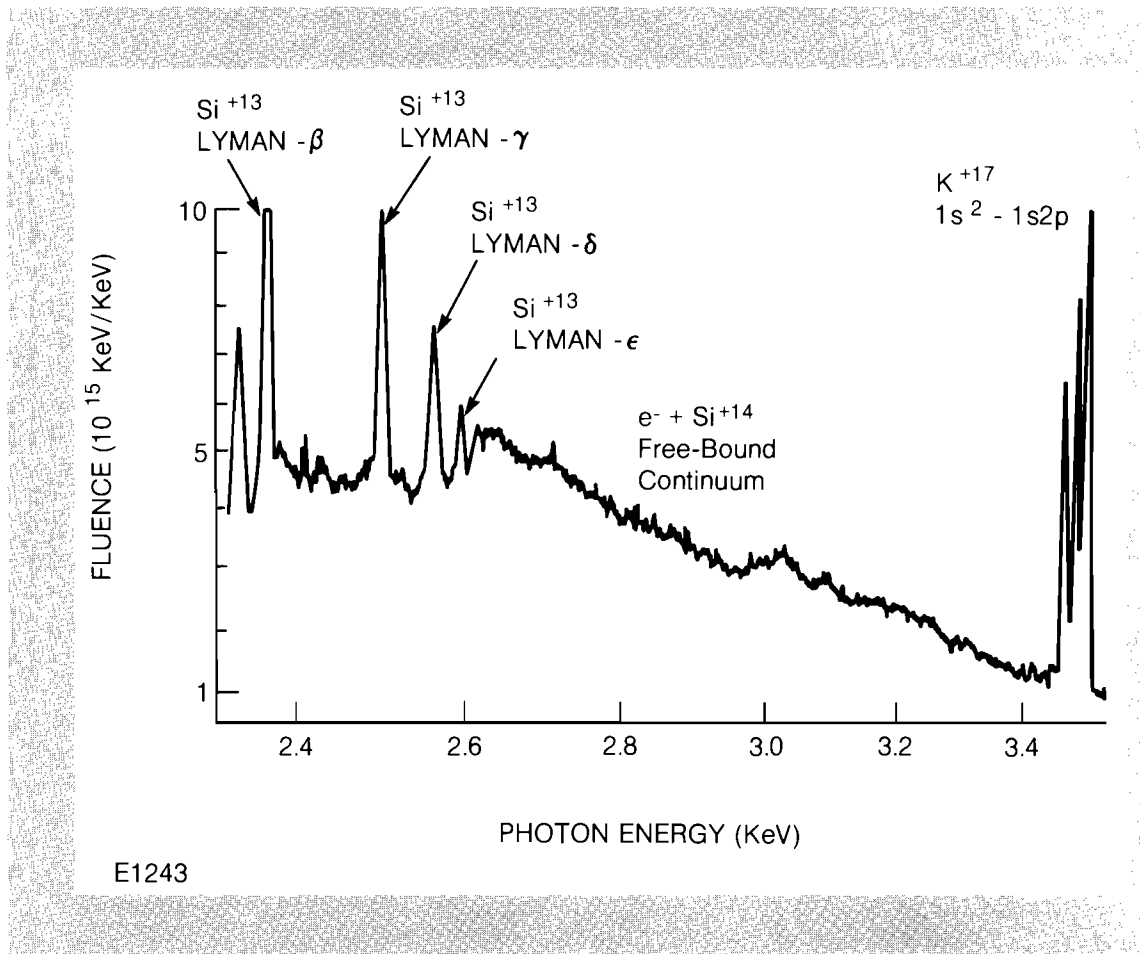


Fig. 13

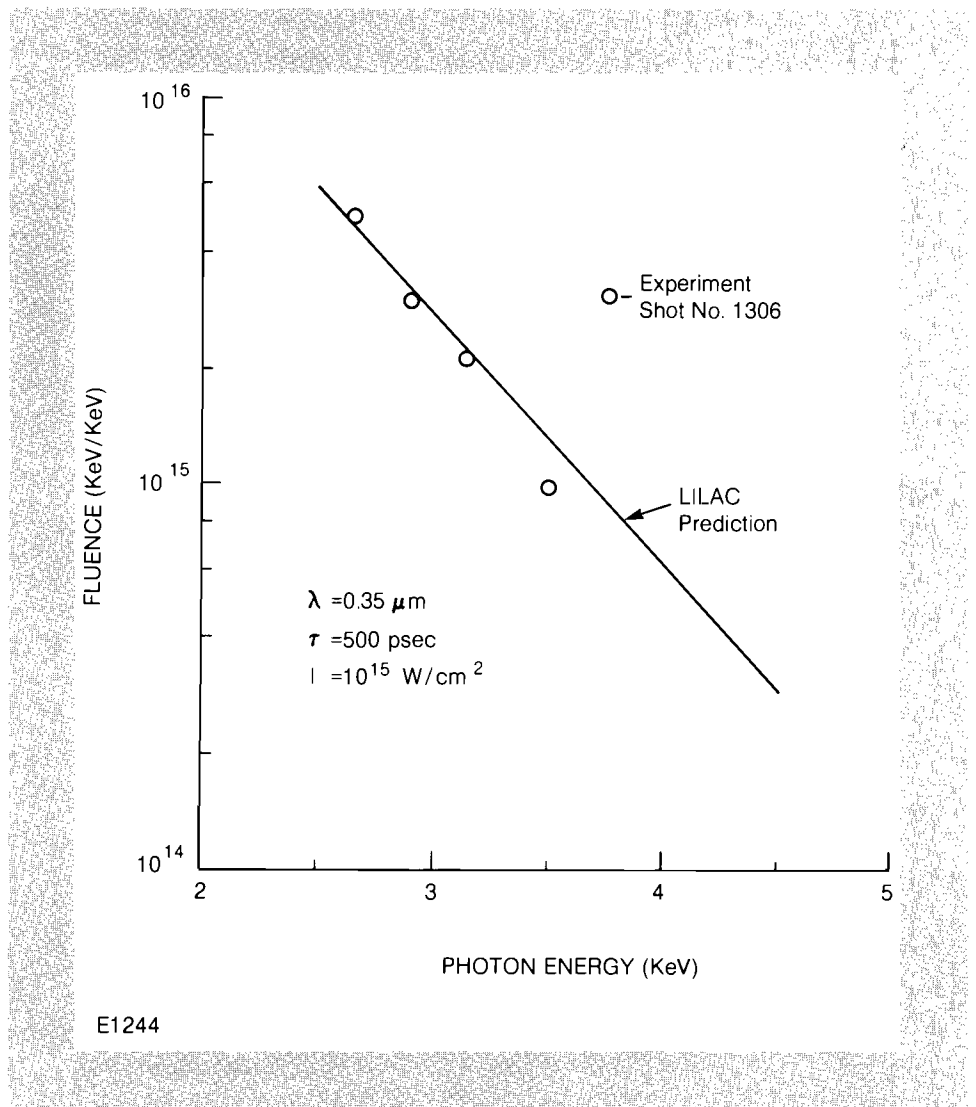
Free-bound x-ray continuum due to the recombination $e^- + \text{Si}^{+14}$ from a glass target irradiated by a $0.35 \mu\text{m}$ laser ($5 \times 10^{14} \text{ W/cm}^2$, 500 psec). Potassium is an impurity in the glass. The strong potassium and silicon lines extend beyond the figure scale. Silicon radiation is emitted at a lower temperature region ($T \sim 0.7 \text{ KeV}$) than that of potassium ($T > 1.5 \text{ KeV}$).

The plasma temperature deduced from the slope of the silicon free-bound continuum is 0.8 KeV. On the other hand, the intensity ratio of the K^{+17} resonance line to the nearby dielectronic satellites¹¹ yields a temperature of about 2 KeV. This difference, completely in agreement with theoretical predictions of the 1D laser fusion code LILAC, is explained by the temperature profile in the target: lines of higher-Z ions are emitted mostly around peak temperature near the critical layer, whereas lines of lower-Z ions come from inside the critical layer where the temperature is

lower. The fact that lower temperature regions lie further inside the target and have a higher density is the main reason for the decrease in line intensity with increasing Z in Fig. 12.

Figure 14 shows a comparison between measured and calculated silicon continuum (from Fig 13). The calculation was performed with LILAC which includes a radiation transport treatment. The target was represented by a sphere of radius twice as large as the laser focal spot, being subjected to the same irradiance as in the experiment (but a higher total energy). The calculated x-ray intensity was then scaled to the measured laser pulse energy. This procedure is known to give best results when trying to simulate the inherently two-dimensional behavior of flat target irradiation by using a spherically symmetric numerical simulation. The agreement with the experiment is very good, in spite of the estimated uncertainty in the experimental absolute values. Further code runs showed the intensity of the silicon continuum to be

Fig. 14
Comparison of measured continuum spectrum (Fig. 13) with prediction of the one-dimensional laser fusion code LILAC. LILAC includes radiation transport treatment.



very nearly linear in the laser irradiance (for a constant target size) over the range $10^{13} - 10^{15}$ W/cm².

A further enhancement of x-ray fluence by an order of magnitude can be expected if UV laser pulses of energy ~ 1 kJ were available and the scaling found here applied at higher intensities. This would mean an irradiance of 10^{14} W/cm² or a fluence of 10^{16} photons in either the resonance line of Si⁺¹² at 1.85 KeV or the integrated silicon continuum in the range $\sim 2.7 - 3.5$ KeV, and 2×10^{15} photons (1.5 J) in the 4.7 KeV line of Ti⁺²⁰. We mention two examples of an application which would be made feasible by such x-ray intensities: (a) the Si⁺¹² resonance line at this irradiance would be capable of resonantly pumping⁷ the $1s^2 - 1s 3p$ transition in Al⁺¹¹ such that gain in the 3-2 transition of Al⁺¹¹ at 4.6 nm may become observable, and (b) for Extended X-ray Absorption Fine-Structure measurements (above an absorption edge)¹² the number of photons above the K-shell edge of, say, Chlorine would be about 10^{10} per resolution element of $\Delta E = 10$ eV at 200 mm from the target, after Bragg diffraction. This would be sufficient to measure EXAFS spectra in systems of dilution down to 100 mM.

REFERENCES

1. W. Seka, S. D. Jacobs, J. E. Rizzo, R. Boni and R. S. Craxton, *Opt. Comm.* **34**, 469 (1980).
2. R. S. Craxton, *Opt. Comm.* **34**, 474 (1980).
3. Annual Report, Ecole Polytechnique, GRECO, 1979; C. E. Max and K. G. Estabrook, University of California, *LLNL Report UCRL-82671-2* (1979), also Comment on Plasma Physics and Controlled Fusion 5, 239 (1980).
4. M. H. Key, C. L. S. Lewis, J. G. Lunney, A. Moore, T. A. Hall and R. G. Evans, *Phys. Rev. Lett.* **41**, 1467 (1978); C. Bayer, D. Billon, M. Decroisette, D. Juraszek, D. Lambert, J. Launspach, M. Louis-Jacquet, J. L. Rocchiccioli and D. Schirmann, *Laser Interaction and Related Plasma Phenomena* (Plenum Press, New York, 1981) 595; D. T. Attwood, N. M. Ceglie, E. M. Campbell, J. T. Larsen, D. M. Matthews, and S. L. Lane, *ibid*, 423; C. Yamanaka, S. Nakai, Y. Kato, T. Sasaki, and T. Mochizuki, 541.
5. R. D. Frankel and J. M. Forsyth, *Science* **204**, 622 (1979).
6. B. Yaakobi, H. Deckman, P. Bourke, S. Letzring, and J. M. Soures, *Appl. Phys. Lett.* **37**, 767 (1980).
7. R. W. Waynant and R. C. Elton, *Proc. IEEE* **64**, 1059 (1976); P. Jaegle, G. Jamelot, A. Carillon, and A. Sureau, to be published in *Lasers* (Marcel Dekker, New York, 1981) Vol. 5; A. V. Vinogradov, I. I. Sobelman, and E. A. Yukov, *Sov. J. Quant. Elect.* **5** 59 (1975); V. A. Bhagavatula, *IEEE J. Q. E.* **QE16**, 603 (1980).
8. R. F. Benjamin, P. B. Lyons, and R. H. Day, *App. Opt.* **16**, 393 (1977).